Ann. For. Res. 65(1): 8132-8143, 2022
ISSN: 18448135, 20652445

ANNALS OF FOREST RESEARCH
https://www.e-afr.org/

A NOVEL ELECTROCHEMICAL ASSAY BASED BIOLOGICAL SYNTHESIS NANOPARTICLES FOR SOME HYDROCARBONS USING SINGLE-STRANDED DNA-BINDING APTAMER

Rand S. Khaleefa[1], Makia M. Al-Hejuje[2] , Hisham F. Mohammad [3]
[1&2] Department of Ecology , College of Science, University of Basrah.
[3] Department of Biology , College of Science, University of Basrah.
*Corresponding author: Rand s. khaleefa +9647703112677
Email:randsalah90@yahoo.com

Abstract
Water samples were collected from Hammar Mushrif plant from three stages to determine the hydrocarbon compounds .A novel electrochemical treatment method was fabricated and modified for rapid, highly sensitive and specific detection of hydrocarbons based on aptamer probe as single-stranded DNA-binding nanoreceptors with electroactive redox probe (Ferrocene) to the surface of screen-printed gold electrode. The results showed six PAHs compounds (Anthracene, B (K) Fluoranthene, IND (1, 2, 3-CD) +Di, B (B) Fluoranthene, pyrene, B (A) pyrene**)** which appeared in three stations before nanotreatment in station 1 their concentrations were (619.71, 23.375, 114.22, 41.221, 17.862, 48.422 mg/l), and in station 2 the concentrations were (488.26, 16.582, 105, 39.509, 18.575, 17.017), while in station 3 the concentrations were (295.31, 13.334, 88.43, 17.336, 10.864, 10.972). The treatment efficiency rang was (2.79% -100%).The designed electrochemical assay exhibited high specificity toward hydrocarbons. Moreover, the developed treating method was successfully applied for removing of target analytes which present in water samples polluted with hydrocarbons.

Keywords: Novel, single-stranded DNA, magnetic iron oxide, carcinogenic hydrocarbons, aptamer.

Introduction

Water is a vital resource for sustaining life, however in present scenario the access to clean safe water around the world has become a burning concern especially in developing and countries attributing to increase in population, climate change and environmental water pollution by sewages, industrial effluents, chemicals, domestic wastes, pesticides, pharmaceuticals (Gonzalez 2012; Uner 2016).

Aquatic resources are among the media most affected by lack of basic sanitation, disposal of plastic wastes and contamination with pesticides, pharmaceuticals, and industrial effluents (Schwarzenbach *et al,* 2010). Industrial effluent is all the liquid waste generated in the various stages of a production process, that is, all the water that is used in an industry and then discarded (A.Al-Ghouti *et al,* 2019). In refining industry, produced water is considered as the largest waste stream, which contains relatively higher concentration of hydrocarbons, heavy metals and other pollutants (A.Al-Ghouti *et al,* 2019). Petroleum hydrocarbons (PHs) are one of the common

© ICAS 2022

contaminants in the environment. They include a broad family of several hundred-hydrocarbon compounds that originally come from crude oil, which is used to make petroleum products. The widespread use of crude oil and other petroleum products for transportation, heating, and industry leads to the release of these petroleum products into the environment through long-term leakage, accidental spills, or operational failure (kadhim *et al*, 2019; Kuppusamy *et al* , 2020). Hydrocarbons differ in their properties according to the number of carbon and hydrogen atoms in the molecule and in the arrangement of atoms. Arrangements including straight chains, branched chains, or cyclic (fused benzene rings) petroleum products also comprises trace amounts of sulfur and nitrogen compounds, which are hazardous and can react with the primary pollutant to produce secondary poisonous chemical (kadhim, 2019). Without proper treatment, the final disposition of produced water can pollute surfaces, groundwater, and soil. Therefore, these components need to reduced or completely removed using some type of treatment including chemical, physical, biological or a combination of two or more of these (Ahmadun *et al*., 2009; Weschenfelder *et al*., 2016; Meneses *et al*., 2017; Al-Ghouti *et al*., 2019). The conventional way of produced water purification before was primarily involve the separation of oil and water physically by making use of gravity and the effluent subsequently dump to the environment (Witze, 2015). The wastewater treatments usually involve three stages, namely primary, secondary, and tertiary treatments, the primary and secondary treatment process is used to removing the majority of large particles and organic matter, respectively. And the tertiary treatment used to remove such matter as a polishing unit (Gedda *et al*., 2021). Nanotechnology-based technology are providing the promising solution because of its extraordinary characteristics like large surface area, low cost maintenance and reuse, etc (Bhati and Rai, 2017). The current water treatment processes are no longer sustainable due to high cost and low efficiency. Due to advantageous properties, nanotechnology based materials can play a great role in increasing the efficiency of water treatment processes (Shah *et al*, 2016). Several methods that can use nanotechnology such as our method, which used as reactive media for separation, filtration, bioremediation and disinfection (Yunus *et al*, 2012).

Material and Methods

Water samples were collected from the Hammar mishrif plant at three stages of treatment. At each stage about (1 L) were collected directly by dark glass bottles for petroleum hydrocarbon analysis.

Hydrocarbon Extraction

Hydrocarbons in water sample from Hammar mishrif before(covenantal treatment) and after Nanotreatment (about 100 ml) were extracted by mixing with another (25 ml) chloroform for 20 min. using separator funnel. The organic (lower) phase was carefully poured into a glass column containing (5g) of anhydrous sodium sulfate (Na_2SO^4), collected and dried by air. The residual was dissolved with n-hexane (25 ml) , and passed through a 20 cm glass column (packed with glass wool at the bottom , about 10 g deactivated silica gel (100-200 mesh), 10 g deactivated

© ICAS 2022

alumina (100-200 mesh) , and 5g anhydrous sodium sulfate (Na_2SO_4) at the top). The aliphatic fractions were eluted from the column with n- hexane (25 ml) , while the aromatics were eluted with benzene (25 ml) .The samples were air dried and stored until detection with Gas chromatography (for aliphatic (n-alkanes) and Gas chromatography-mass for polynucleic aromatic hydrocarbons (PAHs) instruments).

Conventional techniques for treating polluted water:-

The production water treatment unit consists of intermediate produce water IPW, IGF, Nutshell filter N.F. Water is transferred to this unit for separating the water from the oil and is prepared for the purpose of injection into the reservoir. A crossion inhibitor was added to prevent corrosion, a scale inhibitor is added to reduce hardness, and an oxygen scavenger is added, which removes oxygen molecules. In the first stage (IPW), the coagulation process occurs by adding a revece demulsifier that breaks the bonds between water and oil and helps separate oil from water, in the second stage (IGF) separates the remaining oil in small quantities using a polyelectrolyte, a flocculation process occurs, and then the water comes out to (N.F). Filters containing a media of nutshell help separate all the suspended particles in the water. In this way, the treatment process was completed and the water was stored in treated water tanks.

Biogenic Synthesis of Fe_3O_4 nanoparticles

Preparation of plant aqueous extract

The spinach leaf extract (SLE) was used as a biogenic source to make aqueous extracts. Spinach leaves were collected and thoroughly cleaned with distilled water to ensure that they were free of dirt.. To make the plant extract, 20 g of leaves were boiled in 100 mL deionized water for 20 minutes and magnetically stirred at 60° C and then filtered through filter paper. The extract was kept in the fridge for later use.

Biosynthesis of Iron Nanoparticles (FeNPs)

SLE-FeNPs were made by dissolving the $FeCl_3$ in 50 mL of deionized water; a 0.1 M $FeCl_3$ solution was created. FeNPs were synthesized by mixing a 2 : 1 volume ratio of 0.1 M $FeCl_3$ solution with aqueous SLE at 60 °C for 30 minutes with continuous magnetic stirring. As the Fe^{+3} ions decrease, the black color appears. The reaction mixture was prepared in 2 : 1 ratios, and the maximum absorption wavelengths of FeNPs in the UV/visible region were recorded. After that, the mixture was hand-shaken for 1 minute and allowed to sit at room temperature for 1 hour. After 10 minutes, the solution color changed from transparent yellow to dark black, which was noticed and showed in Fig(4). The supernatant was poured out after centrifuging the mixture at 8000 rpm for 30 minutes. The black paste was redispersed in ethanol to remove any remaining biological molecules before being washed with ultrapurified water. To completely purify the NPs, the centrifugation and redispersion in ethanol and ultrapurified water process were repeated three times. The light black paste was then oven-dried overnight at 60 °C, packed, and stored for characterization.

© ICAS 2022

Aptamer Synthesis

Apparatus and reagents

All CV electrochemical measurements were carried out on a DropSTAT2000 potentiostat instrument (from DropSens) controlled by Autolab software using DropSens screen printed gold electrodes (SPGEs). These electrodes have a conventional three electrode configuration with gold working electrode (4-mm diameter disk) and counter electrode (16 mm×1.5 mm curved line), and the potentials were ± 0.2 and ±0.5, at a scan rate of 100mV/s recorded against Ag/AgCl (16 mm×1.5 mm straight line) pseudo-reference electrode.

Aptamer preparation

Single stranded salmon testis DNA (ST ssDNA) were prepared in the lab via QIAGEN extraction kit for animal specimen DNeasy® Blood & Tissue Kit (50) with serial number 69504 which available in website for downloading see www.qiagen.com. The oligonucleotides stock solution was prepared as described by the producer and kept frozen as well as all other chemicals and reagents were of analytical grade and obtained from Sigma.

Immobilization of aptamers

The aptamers were immobilized on gold surface via thiol groups on the 3'- termini in the following procedure. Stock solution of the required aptamer was diluted to 1 μM with HBB or PBB supplemented with 1 mM of 1,4-dithiothretiol (DTT) and 3 mM of $MgCl_2$. DTT causes the removal of the protecting group from the SH moiety and released the aptamers with free SH end groups that could then bind to the surface of screen printed gold electrode in the presence of Mg^{+2} aptamers are initially stretched. Before immobilization, the aptamers samples were activated by rapid (1 min) heating up to 95 °C followed by 1 min cooling at (4 °C) using a conventional thermocycler polymerase chain reaction unit (TECHNE PCR version TC-3000) as appeared in Figure. Immobilization was carried out by casting aptamers solution onto the screen printed gold electrode surface; the samples were then incubated for 4 h at room temperature in a humidity chamber. The unreacted aptamers were removed from the electrode surface by several rinses with non-folding buffer (HBB), then the screen printed gold electrode with immobilized aptamers were kept in HBB to prevent aptamers from coiling.

Electrochemical technique of ssDNA Aptamer

The analytical performances of the ST ssDNA aptamers were compared using two model compounds, Commercial and lab made at the same conditions and concentration. The interaction of the target compounds (PAHs) with the immobilized ST ssDNA aptamer was evaluated by three replicate measurements. After the ST ssDNA immobilization step a drop of 8 μL of the analyte/sample solution was placed onto the work electrode surface for 120 s during the interaction step. Hence the potentiostat analysis was carried out. The variation produced by the analyte interaction was estimated via the percentage of response variation (R%), which is the ratio of the oxidation peak area after the interaction with the sample and the reduction peak area after the

© ICAS 2022

interaction with buffer solution. Evaluation of oxidized beak interaction with immobilized ssDNA and the modification that might occur upon the experimental results of PAHs, two model solutions were tested with UV light at 365 nm for 24 h and were evaluated after UV irradiation using the ssDNA nanoreceptor. 8 µL of the irradiated solutions were placed onto the working electrode surface and after 120 s of incubation a cyclic voltammogram was obtained in the usual conditions. Three replicate measurements were carried out for each investigate concentration level. The designed electrochemical aptasensor needs less than 1 h for detection of hydrocarbons to get these results.

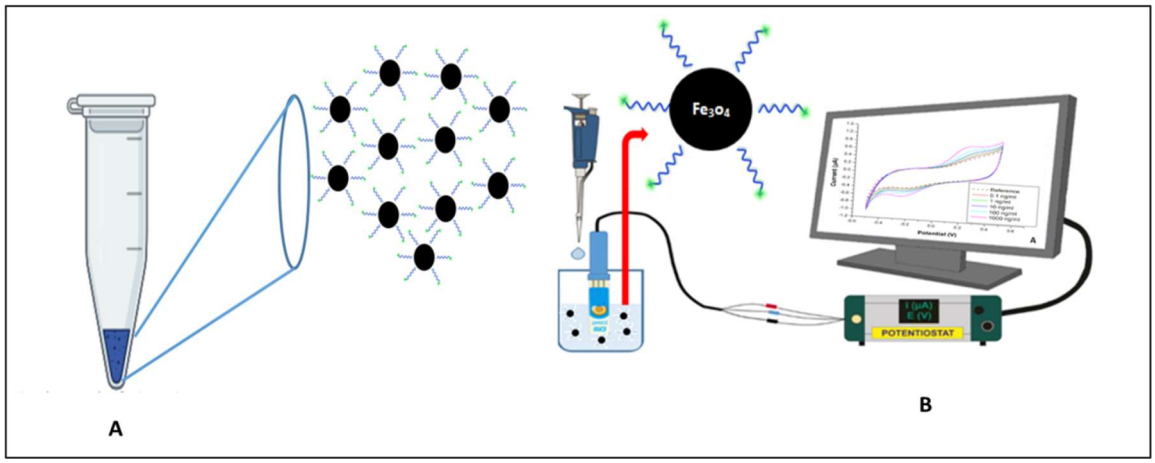

Figure 1: Diagram of Electrochemical assay include (A) Magnetic Iron Oxide nanoparticle and aptamer binding method (B) Detection and isolation of hydrocarbon from water samples.

Experimental Results and Discussions

Fe_3O_4 nanoparticles synthesis

The biogenic synthesized nanoparticles of Fe_3O_4 were formed as shown in image 1.

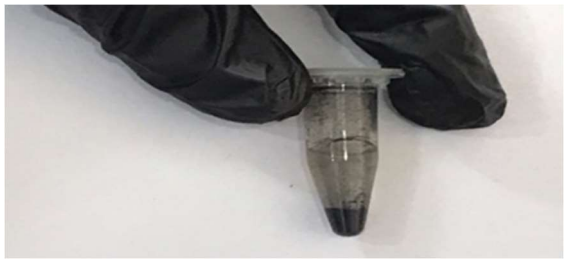

Image 1: Biogenic method of Fe_3O_4 nanoparticles

Fe_3O_4 nanoparticles characterization

The SEM image of Fe_3O_4 nanoparticles was showed in figure 2, also the U.V image was showed in figure 3, in addition to the FTIR , XRD and TEM images were shown in figure 3,4and 5 respectively.

© ICAS 2022

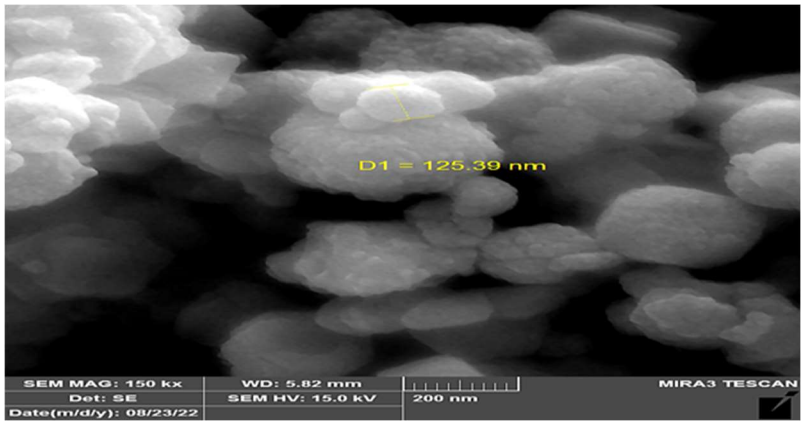

Image 2: FESEM image of Fe_3O_4 nanoparticles

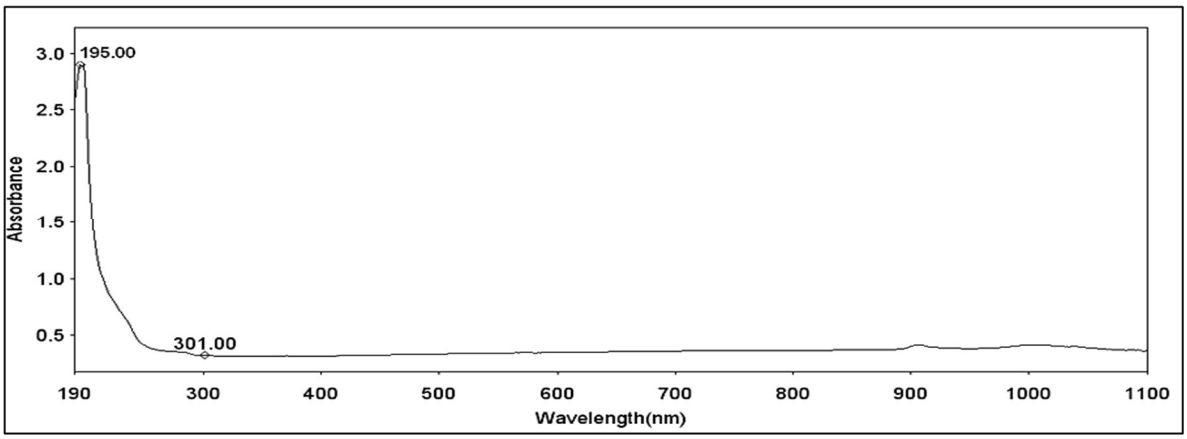

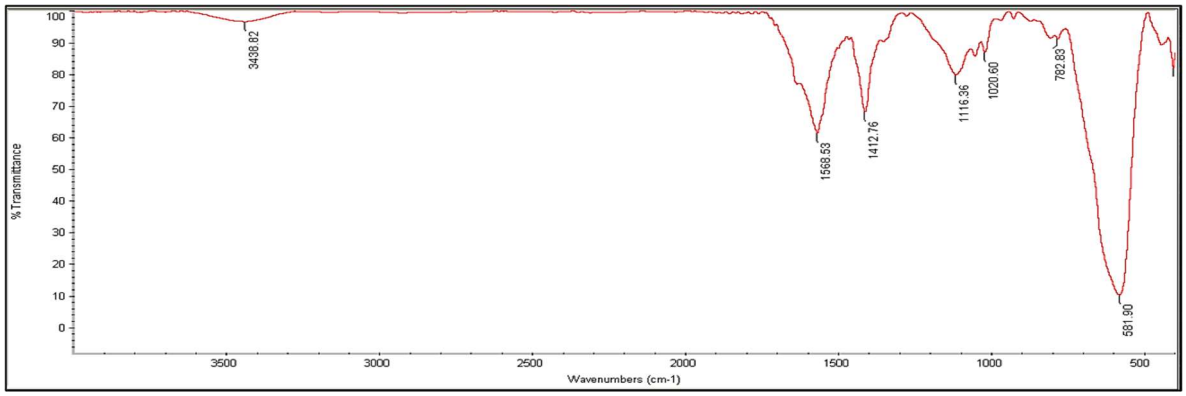

© ICAS 2022

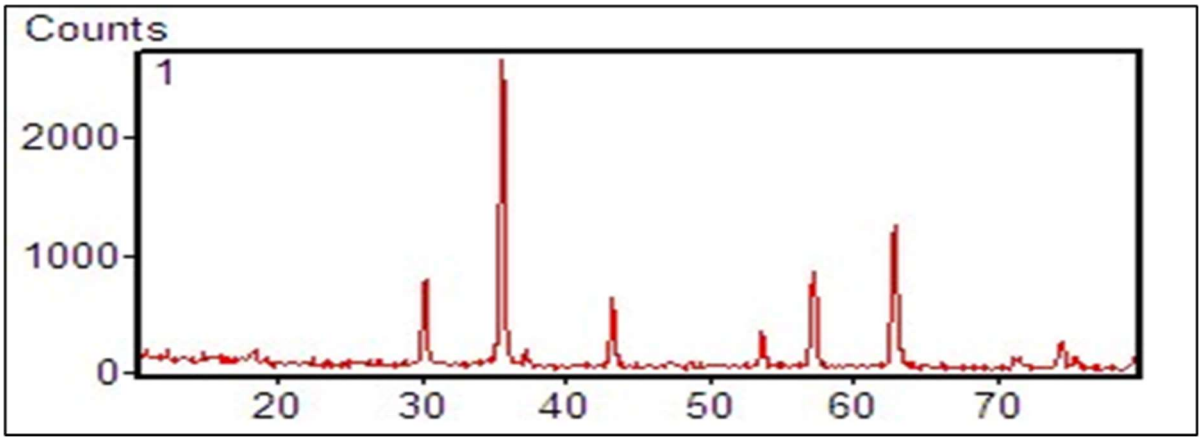

Image 5: XRD spectra of magnetic iron oxide nanoparticles.

Image 6: TEM spectra of magnetic iron oxide nanoparticles.

Electrochemical measurements

The electrochemical strip was immersed in the DNA solution for immobilization onto the screen-printed gold electrode surface at fixed potential of +0.5 V vs Ag screen-printed pseudo-reference electrode for 120 s under stirring. After that a cleaning step was performed by immersion of the strip in a clean acetate buffer solution, at open-circuit for 30 s. Then a potentiometric scan was run to measure the oxidation and reduction peak of the electrode surface by placing 100 µL of analyte. The derivative signal (dt/dE) was recorded versus the potential by using a potential range between 0.5 and (-0.5) V and oxidizing current was 2 µA. The height of the oxidation peak (around +1.05 V vs. Ag screen-printed pseudo-reference electrode) was used as the analytical signal. Three replicate measurements were carried out for each investigate concentration level. Potentiometric behavior was used as the best performing detection techniques in terms of repeatability in comparison to square wave voltammetry and differential pulse voltammetry.

© ICAS 2022

Typical cyclic voltammograms for aptamer (n=3) Before (red peak) and after (blue beak) analyte binding are shown in Figure (2).

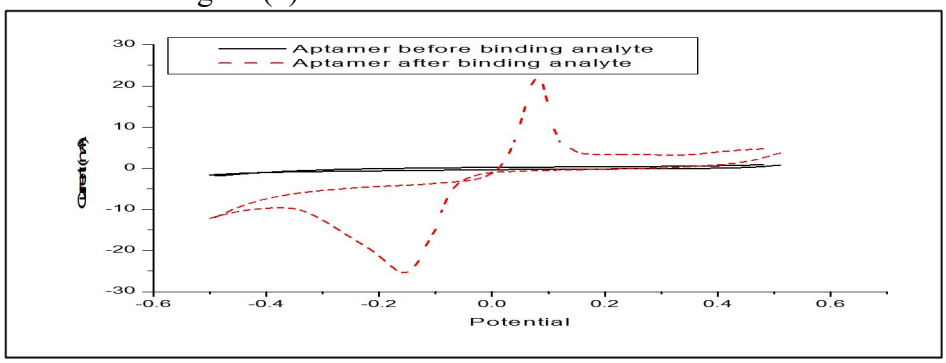

Figure 2 : Cyclic voltammograms of screen-printed gold electrodes with immobilized aptamers in HBB solutions shows the different peaks before and after binding.

The characteristics of the peaks in a cyclic voltammogram can be used to acquire qualitative information about the relative rates of reaction and reactant diffusion in a given electrochemical system. In Figure (2), it can be observed that when the potential of the working electrode is more positive than the reference peak and the current will be increased.

Typical results are shown in Figure (2). As one can see, there is a major difference between these two graphs; in the absence of aptamer binding analyte the current decreased, while in presence of the aptamer binding analyte the current will be almost changed with large increase in values.

Removal of hydrocarbons results

Table (1) The efficiency of hydrocarbons removal:

Compounds	Stations	Concentration conv. treatment	Concentration after nanoteatment	Removal efficiency
Anthracene	ST.1	619.71	130.23	78.99%
	ST.2	488.26	18.42	96.23
	ST.3	295.31	7.71	97.39
Pyrene	ST.1	17.862	17.363	2.79
	ST.2	18.575	0	100
	ST.3	10.864	0	100
B(B)Fluoranthene	ST.1	41.221	12.189	70.43
	ST.2	39.509	15.095	61.794
	ST.3	17.336	0	100
B(K)Fluoranthene	ST.1	23.375	14.471	38.09
	ST.2	16.582	6.035	63.61
	ST.3	13.334	1.181	91.14
B(A)Pyrene	ST.1	48.422	19.488	59.75
	ST.2	17.017	0	100
	ST.3	10.972	0	100

© ICAS 2022

IND.(1,2,3-CD)+Di	ST.1	114.22	91.13	20.22
	ST.2	105	35.06	66.61
	ST.3	88.43	0	100

The results of testing samples with conventional treatment showed that the following compounds did not appear in all stations (Naphthalene, 2-methyl, 1-methyl, Acenaphthyene, Acenaphthnen, fluorine, phenanthrene, Fluoranthene, Chrysene, B (A) Anthracene, Benzo (G, H, I) Perylene, Benzo).

The (Anthracene, B (K) Fluoranthene) compounds appeared in three stations in the conventional treatment with a gradual decrease in concentrations, It also appeared in 3 stations after treatment with a gradual decrease in concentrations between stations after nanotreatment.

The compounds (IND (1, 2, 3-CD) +Di, B (B) Fluoranthene) appeared in the three stations in the conventional treatment with a gradual decrease in concentrations, but they appeared in the first and second stations only after Nano treatment with a gradual decrease in concentrations.

The (pyrene, B (A) pyrene) compounds appeared in the three stations in the conventional treatment with a gradual decrease in concentrations along stations, while they appeared after the nanotreatment only in the first station as showen in table (1). Figure. (3) Showed the percentage of PAHs compounds in water.

The PAHs compounds values in water at the studied stations were illustrated in tables (2). The highest mean concentrations of PAHs in water (499 mg/l) was recorded at station 1 for pyrene, while the lowest mean concentrations (8.904 mg/l) was recorded at station 2 for B (K) Fluoranthene . Non-significant differences ($P>0.05$) were found in station1 for (Anthracene, IND (1, 2, 3-CD) +Di, B (B) Fluoranthene, pyrene, B (A) pyrene) compounds while significant differences ($P<0.05$) were found in station 1 for B (K) Fluoranthene compound.

Non-significant differences ($P>0.05$) were found in station2 for (B (B) Fluoranthene, B (K) Fluoranthene , B (A) pyrene) compounds while significant differences ($P<0.05$)were found in station 2 for (Anthracene, IND (1, 2, 3-CD) +Di, pyrene) compounds.

Non-significant differences ($P>0.05$) were found in station3 for (B (B) Fluoranthene) compound while significant differences ($P<0.05$) were found in station 3 for (Anthracene, IND (1, 2, 3-CD) +Di, pyrene, B (K) Fluoranthene , B (A) pyrene) compounds .

© ICAS 2022

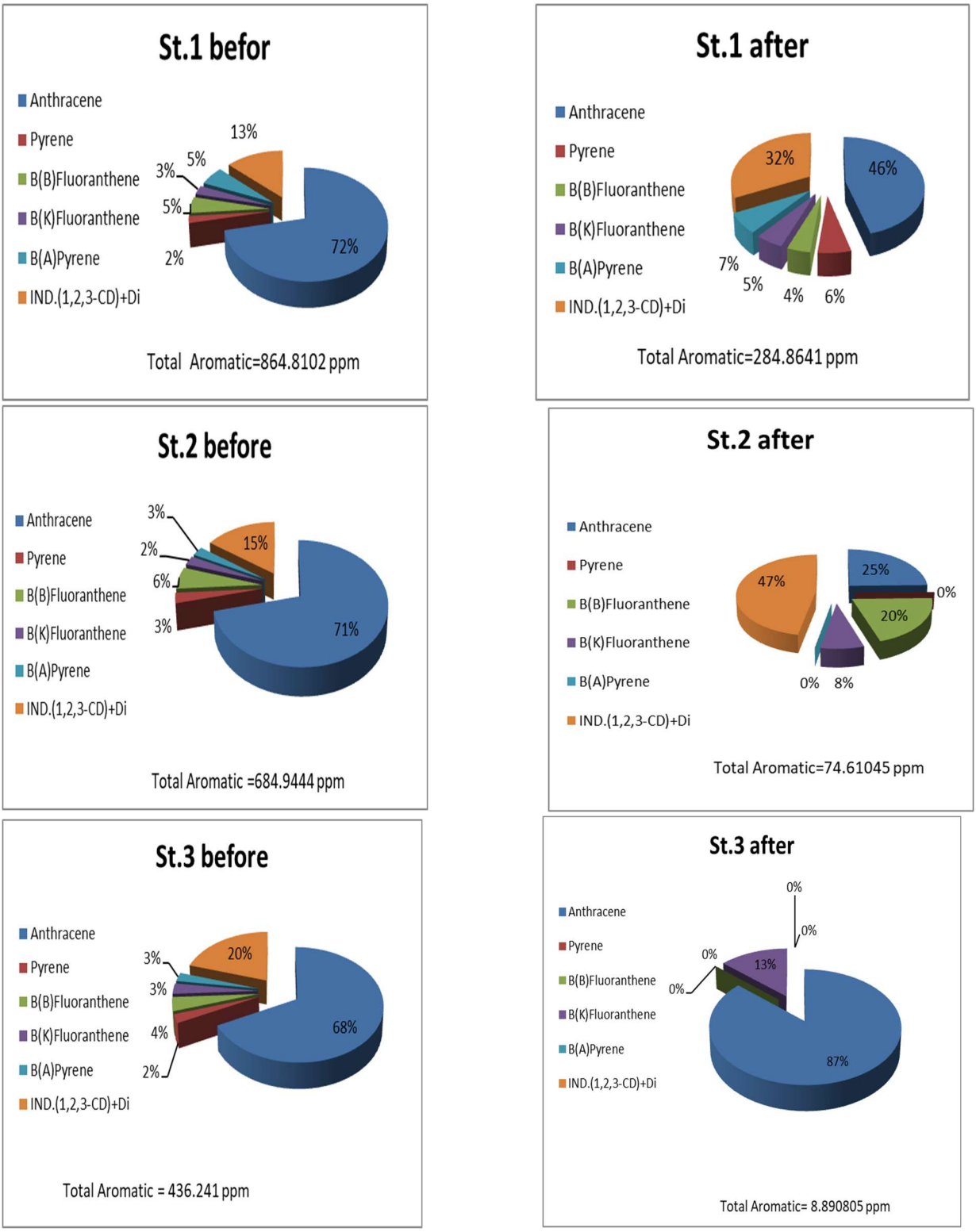

Figure 3. The PAHs compounds percentage in water samples before and after nanotreatment during the studied stations

4. Discussions

The dominant heavy PAHs compounds in water were (Anthracene, B (K) Fluoranthene ,IND (1, 2, 3-CD) +Di, B (B) Fluoranthene, pyrene, B (A) pyrene) were appeared in 3 stages befor nanotreatment this may be related to their high molecular weight that made them settles at the bottom while after nanotreatment some of them treated and not appeared others decreased concentrations because their concentrations were greater than the size of the aptamer, or because the aptamer reached saturation stage. Whereas the dominant light PAHs compounds were Naphthalene, 2-methyl, 1-methyl, Acenaphthyene, Acenaphthnen, fluorine, phenanthrene, Fluoranthene, Chrysene, B (A) Anthracene, Benzo (G, H, I) Perylene, Benzo were undetectable before and after nanotreatment in all stations this may be due to degradation of low molecular weight PAHs in water sample (Bakhtiari *et al*,2009). The results indicates anthropogenic source of PAHs in water sample.

The conformation anti-hydrocarbons aptamer turns to a hair-pin structure accommodating several PAHS compounds, the redox labels come closer to the electrode surface and increase the electron transfer. The increase in concentration of target analyte can increase the concentration of coiled aptamers on the surface and subsequently increase the electrochemical current, in the absence of analyte, SSA interacts with Apt and restricts the access of redox probe to the surface of electrode, leading to a weak current signal. In the presence of target, SSA could not bind to the Apt, resulting in more access of redox probe to the surface of electrode and a strong current signal

5. Conclusion

The concept of electrochemical aptamer binding for hydrocarbons was proved, and the results obtained were encouraging and paving the way for rapid removing method. The selectivity and sensitivity of this aptamer to the PAHs, is promising for development of novel, simple, and cost-effective electrochemical aptamer assay for rapid detection of hydrocarbons in water. A series of cyclic voltammogram measurements allowed the investigation of the mechanism of aptamer/hydrocarbons binding. The proposed model electrochemical aptamer nanoparticle combination based on changing the conformation of aptamer oligonucleotide chain from linear to the folded one, thus bringing the redox label closer to metal surface and increasing the electron charge transfer was proved. A simple detection of anodic (or cathodic) current at fixed voltage corresponding to oxidation (or reduction) peak potential is sufficient for detection of hydrocarbons.

5. References

Ahmadun, F. R., Pendashteh, A., Abdullah, L.C., Biak, D. R. A., Madaeni, S. S., Abidin, Z. Z. Review of technologies for oil and gas produced water treatment. Journal of Hazardous Materials.2009; 170(2- 3): 530-551.

Bakhtiari , A.R. ; Zakaria , M. P. ; Yaziz , M.I. ; Lajis , M.N.H. ; and Bi, X(2009)."Polycyclic Aromatic Hydrocarbons and nalkanes in Suspended Particulate Matter and Sediments from the Langat River , Peninsular Malaysia ". Enviro.Asia , 2 :1-10.

© ICAS 2022

Ian Sofian Yunus , Harwin , Adi Kurniawan , Dendy Adityawarman & Antonius Indarto. Nanotechnologies in water and air pollution treatment, Environmental Technology Reviews.2012; 1:1, 136-148. DOI: 10.1080/21622515.2012.733966.

Gonzalez S, Lopez Roldan R, Cortina JL. Presence and biological effects of emerging contaminants in Llobregat River basin: a review. *Environmental Pollution*. 2012;16:83−92.

Kuppusamy, Saranya; Maddela, Naga Raju; Megharaj, Mallavarapu; Venkateswarlu, Kadiyala .Total Petroleum Hydrocarbons (Environmental Fate, Toxicity, and Remediation);2020 .doi:10.1007/978-3-030-24035-6

M.A. Al-Ghouti, M.A. Al-Kaabi, M.Y. Ashfaq, D.A. Da'na, Produced water characteristics, treatment and reuse: a review, J. Water Process. Eng. 2019; (28)222–239.

Meneses, A. C., Weber, O. B., Crisóstomo, L. A., Andrade, D. J. Biological soil attributes in oilseed crops irrigated with oilfield produced water in the semi-arid region. Revista Ciência Agronômica. 2017; 48(2), 231-241.

Madhulika Bhati & Radhika Rai. Nanotechnology and water purification: Indian know-how and challenges. Environmental Science and Pollution Research.2017; (24)23423–23435.

Nasrullah Shah, Frederick Claessyns , Stephen Rimmer , Muhammad Balal Arain , Touseef Rehan , Aref Wazwaz , Mohammad Wasi Ahmad and Mazhar Ul-Islam. Effective Role of Magnetic Core-Shell Nanocomposites in Removing Organic and Inorganic Wastes from Water. Recent Patents on Nanotechnology.2016; (10)202-212. DOI:10.2174/1872210510666160429145524.

R.P. Schwarzenbach, T. Egli, T.B. Hofstetter, U. von Gunten, B. Wehrli, Global water pollution and human health, Annu. Rev. Environ. Resour. 2010; 35 (1) : 109–136.

Uner O, Gecge lU, Bayrak Y. Adsorption of Methylene Blue by an Efficient Activated Carbon Prepared from Citrullus lanatus Rind: Kinetic, Isotherm, Thermodynamic, and Mechanism Analysis. *Water Air & Soil Pollut.* 2016;227:247

Weschenfelder, S. E., Fonseca, M. J. C., Borges, C. P., Campos, J. C. Application of ceramic membranes for water management in offshore oil production platforms: Process design and economics. Separation and Purification Technology.2016; (171)214-220.

Witze, A. Race to unravel Oklahoma's artificial quakes. Nature2015; 520(7548): 418 – 419.

© ICAS 2022